



Topological manifold immersion based control of parameter uncertain magnetic levitation system

Ali Shahbaz Haider*, Muhammad Babar, Muhammad Zeshaan, Ahmed Aqeel

Department of Electrical Engineering, COMSATS Institute of IT, Wah, Pakistan

ARTICLE INFO

Article history:

Received 27 March 2016

Received in revised form

20 May 2016

Accepted 20 May 2016

Keywords:

Topological manifold

Sub manifold immersion

Nonlinear adaptive control

Magnetic levitation

Parameter uncertain systems

ABSTRACT

This article presents the application of C^∞ topological manifold immersion technique to control parameter uncertain nonlinear dynamic systems in the context of adaptive nonlinear systems theory. The technique is illustrated by implementing it on the challenging unstable nonlinear parameter uncertain magnetic levitation mechanism. The controller design is accomplished by defining a desired reduced order exosystem, whose state space is rendered attractive by a synthesized control law. The unknown system parameters are adaptively estimated. The reference tracking is achieved. The experimental validation of the theoretically proposed controller is presented by implementing discrete time realization of control algorithm using digital controller interfaced in real time with Simulink. The feasibility of the topological manifold immersion based compensation technique is theoretically and experimentally demonstrated by available degrees of freedom in the compensator structure and immense flexibility in the achievable closed loop dynamic.

© 2016 IASE Publisher. All rights reserved.

1. Introduction

Most of the real world systems are nonlinear with parameter uncertainties. The classical linearization techniques result in performance degradation with the parameter uncertainties and also impose the narrow operating range constraints. The topological manifold immersion based control is a new method to design a controller for the nonlinear systems. This technique robustifies a stabilizing controller of a reduced order exosystem, for the given full order system by asymptotically steering the trajectories of full order system to the submanifold of this exosystem. The adaptive nonlinear estimation of the unknown parameters can also be accomplished by the formulations based on the same technique. The classical nonlinear adaptive methods guarantee the estimation error to be bounded but the transient behavior is not well controlled (Yang and Tateishi, 2001). Saturating the unknown parameters to its limiting values may also result in the destabilization of system (Astolfi and Ortega, 2003). However the C^∞ topological manifold immersion technique gives us control on the dynamic behavior of the estimation error response (Luksic et al., 1987). Moreover the resulting adaptive algorithm is stable under the unknown parameter value limits (Maine and Brockett, 1973).

The Magnetic Levitation (maglev) is a challenging system and it is inherently nonlinear and unstable without feedback. It involves suspending a ferromagnetic object such as a steel ball in the space. This setup acts as a benchmark for testing various control techniques (Haider et al., 2015). The topological manifold immersion based control technique is implemented on this system. The reference tracking capability is added in the control algorithm. Simulation has been carried out and the experimental validated of the digitized version of the developed control algorithm is accomplished and results are elucidated.

Organization of the paper is as follows, section 2 describes the main results of the topological manifold immersion method and the adaptive nonlinear parameter estimation. Section 3 gives an overview of the dynamic model of maglev system. Section 4 describes the controller design and the adaptive parameter estimation. Simulation and the experimental validation are presented in section 4, followed by conclusions and discussion in section 5.

2. Topological manifold immersion method

Consider a nonlinear parameter uncertain system:

$$\dot{p} = \underline{s}(p, u_e) = \underline{f}(p) + \underline{g}(p) u_e \quad (1)$$

* Corresponding Author.

Email Address: alishahbaz@ciitwah.edu.pk (A. S. Haider)

where $\underline{p} \in \mathbb{R}^n$ and $u_e \in \mathbb{R}^m$. The state vector \underline{p} evolves on a smooth manifold P of dimension n , which is spanned by tangential manifold to the system map \underline{s} . The system map \underline{s} in Eq. 1 has been decomposed into a drift vector field $\underline{f}(0)$ and a controlled vector field \underline{g} . In Eq. 1, $u_e \in U(P)$ is the system forcing function with U a state dependent input set which belongs to the control bundle $U_{\underline{p} \in P} U(P)$. The topological manifold immersion based nonlinear control approach involves defining a reduced order exosystem. The state trajectories of the exosystem evolve on a C^∞ submanifold $Q \subset P$. The problem of controller design then boiled down to synthesize a control law that dynamically immerses the state trajectories of full order system to the manifold Q . Let us consider an exosystem with state vector $\underline{q} \in \mathbb{R}^q$ with $q < n$, which contains origin in its reachable set. This can be achieved by defining the vector field $\underline{Y}(q)$ of the exosystem that governs the evolution of \underline{q} as given by Eq. 2.

$$\dot{\underline{q}} = \underline{Y}(\underline{q}) \tag{2}$$

Defining a smooth submanifold for the exosystem of Eq. 2 as:

$$Q = \{ \underline{p} \in \mathbb{R}^n | \underline{p} = \underline{\psi}(\underline{q}); \underline{q} \in \mathbb{R}^q \} \tag{3}$$

The controlled integral curves of system map \underline{s} can be attracted by the submanifold Q if partial differential Eq. 4 along with the condition in Eq. 5 is satisfied (Astolfi and Ortega, 2003).

$$\underline{f}(\underline{\psi}(\underline{q})) + \underline{g}(\underline{\psi}(\underline{q})) \wp(\underline{\psi}) = L_{\underline{Y}} \underline{\psi} \tag{4}$$

$$\underline{q}(t) = \underline{0} \forall \underline{q}(0) \in \mathbb{R}^q \text{ as } t \rightarrow \infty \tag{5}$$

Here $L_{\underline{Y}} \underline{\psi} = (\nabla_{\underline{q}} \underline{\psi}) \underline{Y}(\underline{q})$ is the so-called Lie derivative. Also $\wp(\underline{\psi}(\underline{q})) = v(\underline{\psi}(\underline{q})), 0$ on the submanifold Q and $u = v(\underline{P}, \zeta(\underline{P}))$ is the synthesized feedback control law that renders Q attractive. $\zeta(0)$ is the implicit description of Q , which is given by parameterized form in Eq. 6.

$$\zeta(\underline{p}) = \underline{p} - \underline{\psi}(\underline{q}) = 0 \tag{6}$$

Introducing state variable \underline{h} to define "off" the submanifold Q dynamics given by:

$$\dot{\underline{h}} = L_{\underline{s}} \zeta |_{u=\vartheta(\underline{p}, \underline{h})} = \frac{\partial \zeta}{\partial \underline{p}} \underline{s}(\underline{p}, \vartheta(\underline{p}, \underline{h})) \tag{7}$$

In terms of \underline{h} and any constant $\alpha > 0$, the synthesized controller ϑ the system mapping is given by:

$$\dot{\underline{p}} = \underline{s}(\underline{p}, \vartheta(\underline{p}, \underline{h})) \tag{8}$$

For any general system of form:

$$\begin{aligned} \dot{p}_1 &= \xi_1(p_1) + \xi_2(p_1) p_2 \\ \dot{p}_2 &= \varphi(p)^\top \underline{\lambda}_1 + \lambda_2 u \end{aligned} \tag{9}$$

Where $\xi_i(0)$ and $\varphi(0)$ are smooth mappings, λ_i are unknown parameters and $\underline{p}_1 = \xi_1(p_1)$ is globally stable, then for constants $\varepsilon > 0$ and $k > 0$, the geometric adaptive estimates of λ_i are given by (Astolfi and Ortega, 2003),

$$\begin{aligned} \dot{\hat{\lambda}} &= -(I + \nabla_{\hat{\lambda}} \underline{v})^{-1} \left(\nabla_{p_1} \underline{v}(\xi_1(p_1) + \xi_2(p_1) p_2) + \right. \\ &\left. \frac{\partial \underline{v}}{\partial p_2} (-k p_2 - \varepsilon L_{\xi_2} V_1(p_1)) \right) \end{aligned} \tag{10}$$

and the corresponding geomantic synthesized control law is given by:

$$\begin{aligned} u &= -(\hat{\lambda}_2 + v_2(\underline{p}, \hat{\lambda}_1)) \left(k p_2 - \varepsilon L_{\xi_2} V_1(p_1) + \right. \\ &\left. \varphi(p)^\top (\hat{\lambda}_1 + v_1(p)) \right) \end{aligned} \tag{11}$$

The vector $\underline{v} = [v_1(p) \ v_2(\underline{p}, \hat{\lambda}_1)]^\top$ is given by:

$$v_1(p) = \gamma_1 \int_0^{p_2} \varphi(p_1, \eta) d\eta \tag{12}$$

$$\begin{aligned} v_2(\underline{p}, \hat{\lambda}_1) &= \gamma_2 \left(k \frac{p_2}{2} - \varepsilon L_{\xi_2} V_1(p_1) p_2 \right) + \\ &\gamma_2 \int_0^{p_2} \varphi(p_1, \eta)^\top (\hat{\lambda}_1 + v_1(p_1, \eta)) d\eta \end{aligned} \tag{13}$$

Where $V_1(p_1)$ is any mapping such that for some class-K function $K(0)$, we have (Jurdjevic, 1996),

$$L_{\xi_1} V_1(p_1) \leq -\kappa(p_1) \tag{14}$$

and $\gamma_2 > 0, \gamma_2 > 0$ are constants.

3. The dynamic model of maglev system

The hardware platform of the maglev system is shown in Fig. 1. It consists of an electromagnets and a steel ball. In free air ball drops down under the action of gravity so electromagnet is used to provide counter gravity force. A bulb and solar panel assembly is used to sense the position of the steel ball in air. Fig. 2 shows the EM coil equivalent circuit and free body diagram of the EM coil. The state vector for the Maglev system is defined in Eq. 15.

$$\underline{p} = [p_1 \ p_2 \ p_3]^\top = [y \ \dot{y} \ i]^\top \tag{15}$$

For the maglev system various system mappings in Eq. 1 can be express by Eq. 16 (Haider et al., 2015; Brogan, 1985).

$$\begin{aligned} \underline{f}(\underline{p}) &= [p_2 \ -k_1 + k_2 p_3^2/p_1 \ -p_3 k_3]^\top \\ \underline{g}(\underline{p}) &= [0 \ 0 \ k_4]^\top \end{aligned}$$

$$\underline{s}(\underline{p}, u_e) = [p_3 \quad -k_1 + k_2 p_3^2/p_1 \quad -p_3 k_3 + k_4 u_e]^T \quad (16)$$

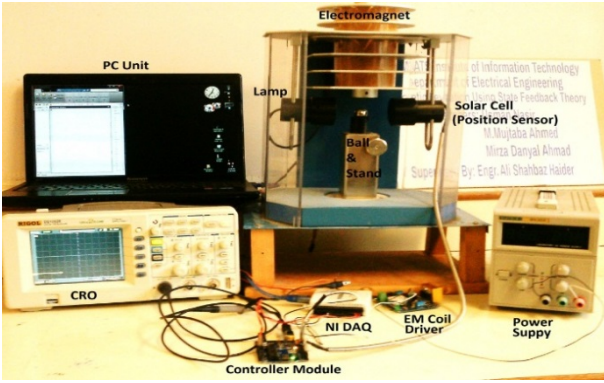


Fig. 1: The experimental setup

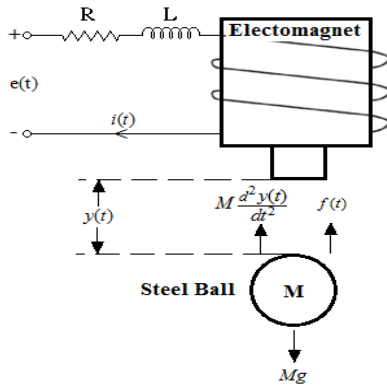


Fig. 2: The equivalent circuit of electromagnet and the free body diagram

Here $k_1=g$, $k_3=R/L$, $k_4=1/L$ and $k_2 = g p_{01}/p_{03}^2$. The value of the acceleration due to gravity g is treated as an unknown parameter with the known bounds. The value of the parameter $k_2 = g p_{01}/p_{03}^2$ depends upon a particular operating point (p_{01}, p_{03}) , hence it is also treated as an unknown parameter while designing compensator.

4. Controller design and parameter estimation

Using the results of section 2 and the maglev model of section 3, we can define the mappings $\underline{Y}(0)$ and $\underline{\psi}(0)$ in Eq. 17 and Eq. 18 respectively.

$$\underline{\psi}(q) = [q_2 \quad -k_1 + k_2 \zeta_1^2/q_1]^T \quad (17)$$

$$\underline{p} = \underline{\psi}(q) = [q_1 \quad q_2 \quad \psi_1(q_1, q_2)]^T \quad (18)$$

The solution of Eq. 4 through Eq. 8 gives us full information controller of Eq. 19, where the term ζ_1 in the control law is yet to be synthesized.

$$\vartheta(\underline{p}, \hat{h}) = \frac{-\alpha \hat{h} + \zeta_1 + k_3 p_3}{k_4} \quad (19)$$

The system in Eq. 8 takes the form:

$$\dot{\hat{h}} = -\alpha \hat{h}$$

$$\dot{p}_1 = p_2$$

$$\dot{p}_2 = -k_1 + k_2 \zeta_1^2/p_1$$

$$\dot{p}_3 = -\alpha \hat{h} + \zeta_1 \quad (20)$$

If the control law ζ_1 is stabilizing then it is evident that as $t \rightarrow \infty$ the state trajectories of full order system Eq. 20 immerse from manifold P to the submanifold Q.

5. Nonlinear adaptation of unknown parameters

From Eq. 20, the exosystem evolving on the submanifold Q is given by Eq. 21.

$$\dot{p}_1 = p_2$$

$$\dot{p}_2 = -k_1 + k_2 \zeta_1^2/p_1 \quad (21)$$

If we define the stabilizing controls law as:

$$\zeta_1 = \sqrt{|u p_1|} \quad (22)$$

Then exosystem in Eq. 21 takes the form of Eq. 23, with unknown parameters k_1 and k_2 .

$$\dot{\underline{p}}_1 = [p_2 \quad -k_1 + k_2 u]^T \quad (23)$$

Comparing Eq. 9 and Eq. 23 and assuming "control polarity" to be positive we get:

$$\underline{\xi}_1(\underline{p}_1) = 0, \quad \underline{\xi}_2(\underline{p}_1) = 1$$

$$\lambda_1 = k_1, \quad \lambda_2 = k_2 > 0$$

$$\varphi(\underline{p}) = -1 \quad (24)$$

Defining $V_1(\underline{p}_1) = p_1^2$ satisfies Eq. 14 as:

$$L_{\underline{\xi}_2} V_1(\underline{p}_1) = 2p_1 \quad (25)$$

Using Eq. 24 through Eq. 25 and Eq. 12-13, \underline{v} evaluates to be:

$$\underline{v} = \begin{bmatrix} c_1 p_2 \\ c_2 p_2^2 + c_3 \hat{\lambda}_1 p_2 + c_4 p_1 p_2 \end{bmatrix} \quad (26)$$

Where $c_1 = -\gamma_1$, $c_2 = 0.5(k\gamma_2 + \gamma_1\gamma_2)$, $c_3 = -\gamma_2$ and $c_4 = 2\varepsilon\gamma_2$. We have:

$$\nabla_{\underline{\lambda}} \underline{v} = \begin{bmatrix} 0 & 0 \\ -\gamma_2 p_2 & 0 \end{bmatrix} \quad (27)$$

$$\nabla_{p_1} \underline{v} = \frac{\partial \underline{v}}{\partial p_1} = [0 \quad 2\varepsilon\gamma_2 p_2]^T \quad (28)$$

$$\frac{\partial \underline{v}}{\partial p_2} = [-\gamma_1 \quad k\gamma_2 p_2 + 2\gamma_2 k p_1 - \gamma_2 \hat{\lambda}_1 + \gamma_2 \gamma_2 p_2] \quad (29)$$

Using Eq. 27 through Eq. 29, the parameter estimates of Eq. 10 evaluate to Eq. 30.

$$\dot{\hat{\lambda}} = \begin{bmatrix} c_5 p_1 + c_6 p_2 \\ c_7 p_1^2 + c_8 p_2^2 + c_9 p_1 p_2 + c_{10} p_2 \hat{\lambda}_1 + c_{11} p_1 \hat{\lambda}_1 \end{bmatrix} \quad (30)$$

and the control law of Eq. 11 evaluates to Eq. 31.

$$u = -\left(\hat{\lambda}_2 + v_2(p, \hat{\lambda}_1)\right)\left(kp_2 + 2\epsilon p_1 - \hat{\lambda}_1 - v_1(p)\right) \quad (31)$$

The various constants in Eq. 30 are $c_5 = -2\epsilon\gamma_2$, $c_6 = -k\gamma_2$, $c_7 = 4\gamma_2\epsilon^2$, $c_8 = -2\epsilon\gamma_1 + \gamma_1\gamma_2k$, $c_9 = -2\gamma_2^2\epsilon + 2\gamma_1\gamma_2\epsilon$, $c_{10} = -\gamma_2k$ and $c_{11} = -2\gamma_2\epsilon$. To achieve reference tracking for the position of the ball, we modify the control algorithm of Eq. 19 as:

$$\vartheta_1(p, \hat{h}) = \frac{-a\hat{h} + \zeta_1 + k_3 p_3}{k_4} + \sigma(t) \quad (32)$$

For a reference signal $r(t)$, error signal is defined as:

$$e(t) = r(t) - p_1(t) \quad (33)$$

The function $\sigma(t)$ in Eq. 32 is given by:

$$\sigma(t) = \Xi(e(t)) \quad (34)$$

Where $\Xi(0)$ is the control law to achieve the desired transient response for the reference tracking? We have selected proportional-derivative action with proper scaling and gains as:

$$\Xi(t) = -\frac{k_3}{k_4}\left(k_p(\cdot) + k_d \frac{d(\cdot)}{dx}\right) \quad (35)$$

6. Simulation and experimental results

The system has been simulated in the Simulink as shown in Fig. 3. The values of various parameters are given in Table 1. The grey shaded blocks in Fig. 3

correspond to the plant and white background blocks correspond to the control and estimation algorithms. Fig. 4 shows the Simulink model that implements the control and estimation algorithm in real time by operating the plant in Rapid Control Prototyping (RCP) mode. The Real time data is collected by ARM Cortex-M3 processor. It is processed in Simulink and manipulated signal is passed on to the plant. The RCP capability enables to tune the control and estimation algorithm parameters in real time for the desired response hence speeding up the design process. The expended view of the reference tracker control law block is shown in Fig. 5. The value of both gain parameters, namely k_p and k_d is tuned at Fig. 5. Fig. 6 shows the simulated reference tracking response of the position of the ball and the corresponding responses of the velocity of the ball and the EM coil current. The response is stable and the position of the ball tracks well the reference signal with zero steady state error. Fig. 7 shows the input voltage signal to the EM coil.

Fig. 8 shows the immersion of full order system state trajectories to the submanifold Q . The trajectories of the both simulated and experimental data are shown.

Fig. 9 through Fig. 12 shows the experimental results. Fig. 9 shows the response of the position of the ball to a pulse train reference signal. The response shows some overshoot but stabilizes with zero steady state error.

Fig. 10 shows the response of the velocity of the ball to a pulse train reference for the position of the ball. Fig. 11 shows the experimental response of the EM coil current that is measured using Hall Effect sensor. Fig. 12 shows the experimental response of the EM coil input voltage that is the manipulation signal generated by the control and estimation algorithm.

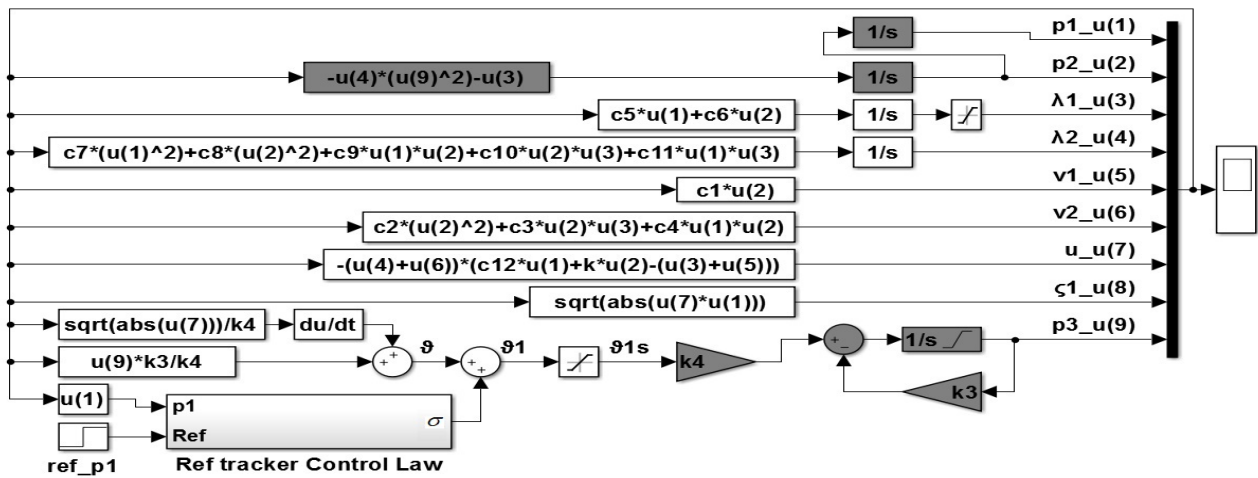


Fig. 3: The RCP mode of operation for MagLev system controller tuning and experimental validation

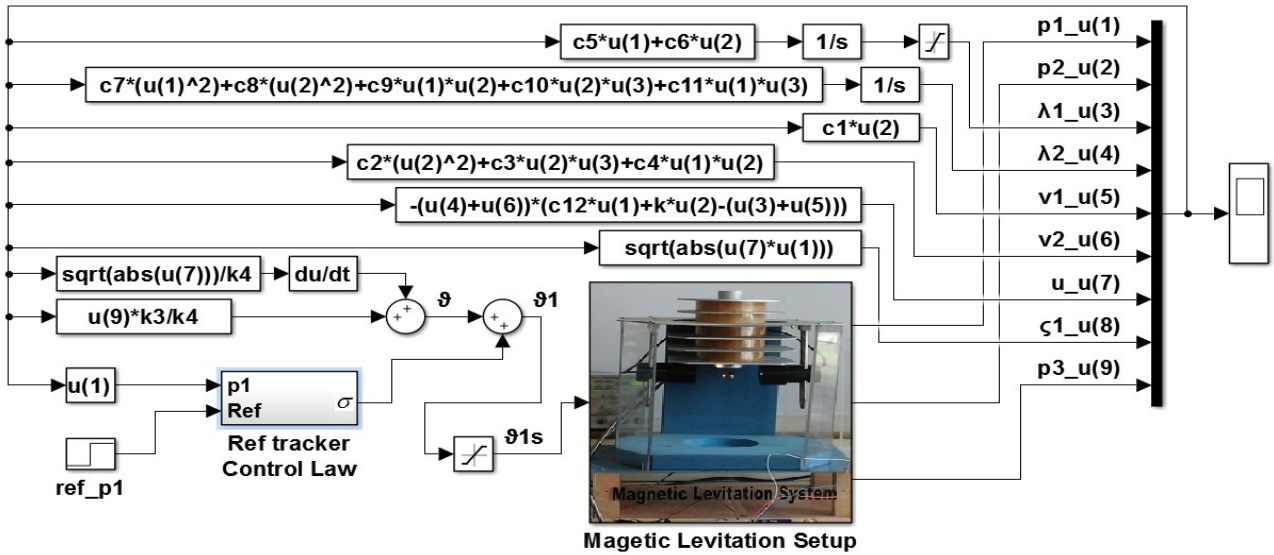


Fig. 4: The Simulink model of MagLev system

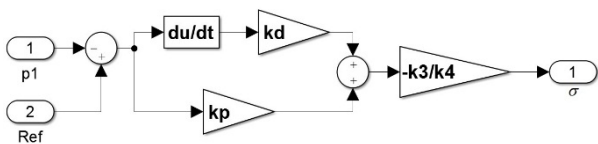


Fig. 5: Expanded view of the reference tracker control law block

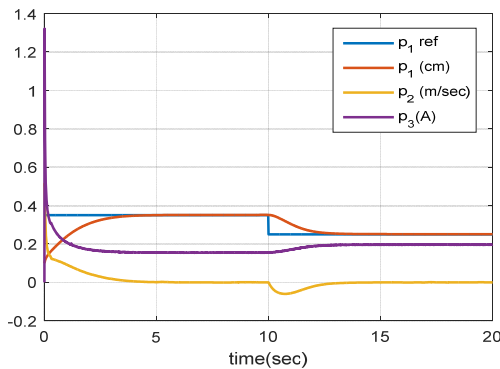


Fig. 6: Simulation responses of Maglev system states.

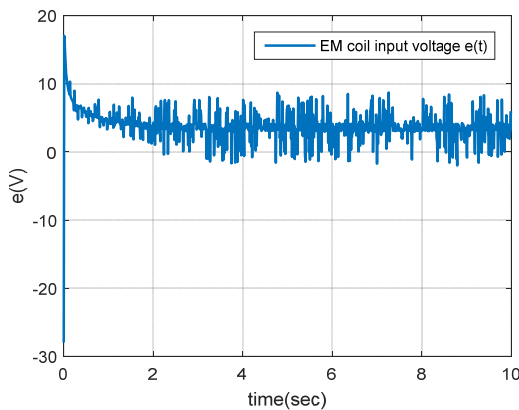


Fig. 7: The EM coil input voltage.

7. Discussion and conclusions

The manifold immersion based nonlinear control approach for the compensator design of a parameter uncertain MagLev system has been presented. The uncertain parameters are adaptively estimated. This

approach is successful in attaining the desired position of the ball in the air. The manifold immersion based approach provides immense degree of freedom in selecting the desired closed loop dynamics owing to the availability of free tunable variables in the stabilizing control algorithm. The proposed algorithm is successful in attracting the state trajectories of full order system to the reduced order desired submanifold. The successful reference tracking for the position of the ball from any initial condition, within the actuating signal range limits, is achieved. The experimental results show the promising performance of the plant.

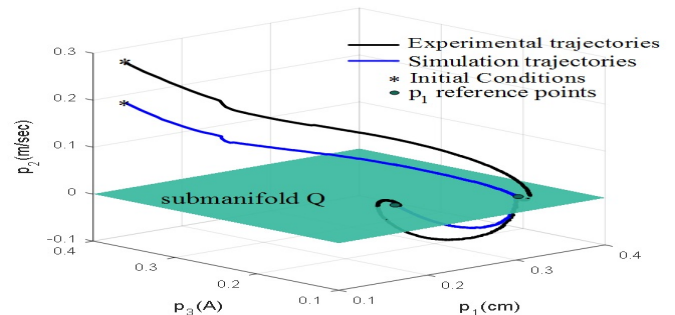


Fig. 8: The trajectories of MagLev system

Table 1: Values of the system parameters

Parameter	Value	Parameter	Value
k_3	137.5	c_4	0.004
k_4	6.14	c_5	-0.004
k	80.0	c_6	-160
γ_1	5.00	c_7	8×10^{-6}
γ_2	1.00	c_8	799.99
ε	1×10^{-3}	c_9	0.0120
c_1	-5.0	c_{10}	-160.0
c_2	85.0	c_{11}	-0.004
c_3	-2.0	c_{12}	0.002

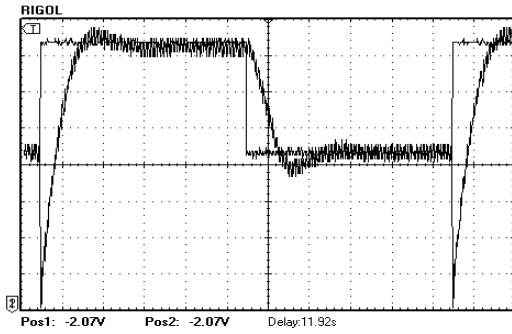


Fig. 9: Experimental response of the position of the ball

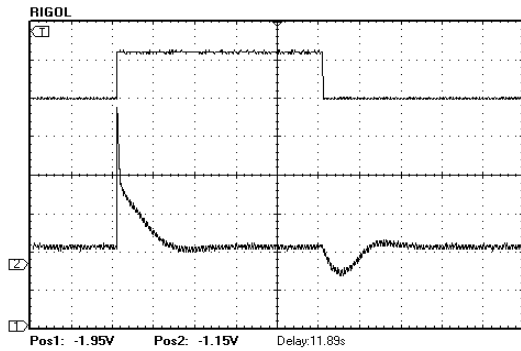


Fig. 10: Experimental response of the velocity of the ball: ball position reference signal (top), velocity of the ball (bottom)

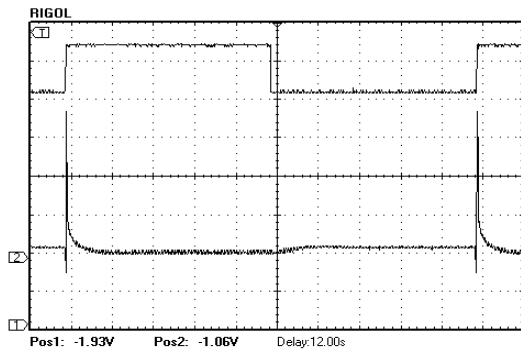


Fig. 11: Experimental response of the EM coil current: ball position reference signal (top), EM coil current (bottom)

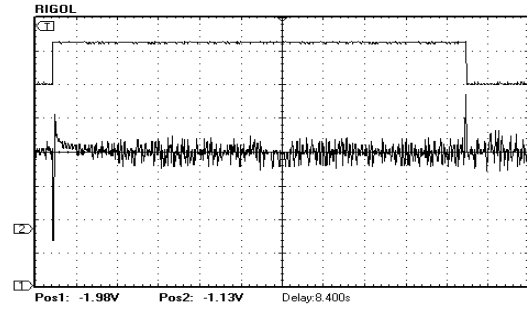


Fig. 12: Experimental response of the EM coils input voltage: ball position reference signal (top), EM coil input voltage (bottom).

References

- Astolfi A and Ortega R (2003). Immersion and Invariance: a new tool for stabilization and adaptive control of nonlinear systems. *IEEE Trans. on Automatic Control*, 48(4): 590–606.
- Brogan WL (1985). *Modern Control Theory*. Prentice Hall. New Jersey, USA.
- Haider AS, Nasir U, Mujtaba M, and Ahmed MD (2015). Controller Design for Magnetic Levitation System Using Diophantine Minimum Order Estimator Approach. *ICGST-ACSE Journal*, 15(2): 1-8.
- Jurdjevic V (1996). *Geometric Control Theory*. Cambridge University Press. Cambridge, UK.
- Luksic M, Martin C and Shadwick W (1987). *Differential Geometry: The Interface between Pure and Applied Mathematics*. American Mathematical Society, Providence. R.I, USA.
- Maine DQ and Brockett RW (1973). *Geometric Methods in Systems Theory*. D. Reidel Publishing Company. Dordrecht, Netherlands.
- Yang ZJ and Tateishi M (2001). Adaptive robust nonlinear control of a magnetic levitation system. *Automatica*, 37(7): 1125–113.